Focussed on: Fracture and Structural Integrity related Issues

Fatigue crack behavior on a Cu-Zn-Al SMA

V. Di Cocco, F. Iacoviello
Università di Cassino e del Lazio Meridionale, DICeM, Via G. Di Biasio, 43, 03043, Cassino (FR), Italy
v.dicocco@unicas.it

S. Natali, V. Volpe
University of Rome "Sapienza", DICMA, Via Eudossiana 18, Rome, Italy
stefano.natali@uniroma1.it

ABSTRACT. In recent years, mechanical property of many SMA has improved in order to introduce these alloys in specific field of industry. Main examples of these alloys are the NiTi, Cu-Zn-Al and Cu-Al-Ni which are used in many fields of engineering such as aerospace or mechanical systems. Cu-Zn-Al alloys are characterized by good shape memory properties due to a bcc disordered structure stable at high temperature called β-phase, which is able to change by means of a reversible transition to a B2 structure after appropriate cooling, and reversible transition from B2 secondary to DO3 order, under other types of cooling. In β-Cu-Zn-Al shape memory alloys, the martensitic transformation is not in equilibrium at room temperature. It is therefore often necessary to obtain the martensitic structure, using a thermal treatment at high temperature followed by quenching. The martensitic phases can be either thermally-induced spontaneous transformation, or stress-induced, or cooling, or stressing the β- phase. Direct quenching from high temperatures to the martensite phase is the most effective because of the non-diffusive character of the transformation. The martensite inherits the atomic order from the β-phase. Precipitation of many kinds of intermetallic phases is the main problem of treatment on cu-based shape memory alloy. For instance, a precipitation of α-phase occurs in many low aluminum copper based SMA alloy and presence of α-phase implies a strong degradation of shape recovery. However, Cu-Zn-Al SMA alloys characterized by aluminum contents less than 5% cover a good cold machining and cost is lower than traditional NiTi SMA alloys. In order to improve the SMA performance, it is always necessary to identify the microstructural changing in mechanical and thermal conditions, using X-Ray analyses.
In this work a Cu-Zn-Al SMA alloy obtained in laboratory has been microstructurally and metallographically characterized by means of X-Ray diffraction and Light Optical Microscope (LOM) observations. Furthermore a fatigue crack propagation and fracture surface scanning electron microscope (SEM) observations have been performed in order to evaluate the crack path and the main crack micromechanisms.

KEYWORDS. SMA; Cu alloys; Structure; Fatigue crack propagation.

INTRODUCTION

Since the discovery of the first shape memory alloy (Au-Cd, in 1938), many alloys characterized by memory property have been studied. Often, the chemical composition was characterized by the presence of rare metals with low mechanical properties and SMA effects that did not allow an industrial development on a large scale. In recent

years, mechanical properties of many SMA have improved, allowing to introduce these alloys in specific field of industry. Main examples of these alloys are the NiTi, Cu-Zn-Al and Cu-Al-Ni which are used in many fields of engineering such as aerospace or mechanical systems [1].
Many scientific papers are published mainly on NiTi alloy (Nitinol), analyzing both the microstructure peculiarities and the thermo-mechanical properties [2]. However, this alloy is characterized by some processing difficulties that imply an increase of costs. The main difficulty is due to presence of titanium that makes it readily oxidisable and, because of its good mechanical properties, it must be hot worked.
In the last decades, different shape memory alloys have been optimized, such as the copper-zinc-aluminum (ZnCuAl), copper-aluminum-nickel (CuAlNi), nickel-manganese-gallium (NiMnGa), nickel-titanium (NiTi), and other SMAs obtained alloying zinc, copper, gold, iron, etc.. However, the near equiatomic NiTi binary system shows the most interesting properties and it is currently used in an increasing number of applications in many fields of engineering, for the realization of smart sensors and actuators, joining devices, hydraulic and pneumatic valves, release/separation systems, consumer applications and commercial gadgets [1, 2]. Due to their good biocompatibility, another important field of SMA application is medicine, where the pseudo-elasticity is mainly exploited for the realization of several components such as cardiovascular stent, embolic protection filters, orthopedic components, orthodontic wires, micro surgical and endoscopic devices [3].
From the microstructural point of view, shape memory and pseudo-elastic effects are due to a reversible solid state microstructural transition from austenite to martensite, which can be activated by mechanical and/or thermal loads [4].
Copper-based shape-memory alloys are very sensitive to thermal effects, and it is possible that in thermal cycles its properties change (e.g., shape-recovery ratio, transformation temperatures, crystal structures, hysteresis and mechanical behavior).
Cu-Zn-Al alloys are characterized by good shape memory properties due to a bcc disordered structure stable at high temperature called β-phase, which is able to change by means of a reversible transition to a B2 structure after appropriate cooling, and reversible transition from B2 secondary to DO3 order, under other types of cooling. In β-Cu-Zn-Al shape memory alloys, the martensitic transformation is not in equilibrium at room temperature. It is therefore often necessary to obtain the martensitic structure, using a thermal treatment at high temperature followed by quenching. The martensitic phases can be either thermally-induced spontaneous transformation, or stress-induced, or cooling, or stressing the β-phase. Direct quenching from high temperatures to the martensite phase is the most effective because of the non-diffusive character of the transformation. The martensite inherits the atomic order from the β-phase [5].
Precipitation of many kinds of intermetallic phases is the main problem of treatment on Cu-based shape memory alloy. For instance, a precipitation of α-phase occurs in many low aluminum copper based SMA alloy and presence of α-phase implies a strong degradation of shape recovery [6]. However, Cu-Zn-Al SMA alloys characterized by aluminum contents less than 5% cover a good cold machining and cost is lower than traditional NiTi SMA alloys.
Other investigations carried out on CuZnAl alloys, showed a strain influence on the macroscopic behavior and on martensite morphology. Martensitic transformation occurs initially in deformed material and the manufact shape follows the transformation [7]. Larger grains dimensions allow an easier transformation process, allowing the growth of 18R martensite [8].
In this work a Cu-Zn-Al SMA alloy obtained in laboratory has been microstructurally and metallographically characterized by means of X-Ray diffraction and Light Optical Microscope (LOM) observations. These analyses have performed under load conditions in order to identify the behavior of alloy. Furthermore fatigue crack propagation and fatigue crack paths were investigated by means of a scanning electron microscope (SEM).

MATERIAL AND PROCEDURES

In this work, a CuZnAl pseudo-elastic alloy, made in laboratory by using controlled atmosphere furnace and characterized by chemical composition shown in Tab. 1, has been investigated focusing the fatigue crack propagation paths.

Cu	Zn	Al	Other
73.00	21.80	5.04	0.16

Table 1: Chemical composition of Cu-Zn-Al investigated alloy.

Prior to evaluate mechanical properties, crono-amperometric tests have been performed in order to evaluate the homogeneity of material and its electrochemical behaviours, using a 0.1 mol NaCl solution at -50mV/SCE for 1800s [9].
In order to evaluate the structure transformation, a customized testing machine equipped with a removable loading frame was used to perform X-Ray analyses at fixed values of applied load and/or deformations. XRD measurements were carried out by using a Philips X-PERT PRO diffractometer equipped with vertical Bragg-Brentano powder goniometer. A step-scan mode was used in the 2θ range from 25° to 90° with a step width of 0.02° and a counting time of 3 s per step, and receiving slit 0.02 mm. The employed radiation was monochromated Cu Kα (40kV – 40 mA).
Fatigue crack propagation tests were performed by using CT specimens obtained by machining the cast ingots according to ASTM E 647 prescriptions. Both lateral surfaces have been metallographically prepared to Scanning Electron Microscope (SEM) observations. A servohydraulic testing machine has been used in order to evaluate fatigue crack propagation using the ASTM E 647 testing conditions.
Fatigue cracks propagation tests are performed by using the following conditions:

1) ΔP = const.
2) $R = P_{min}/P_{max}$ = 0.1 and 0.5.
3) Load: Sinusoidal waveform.
4) Load frequency = 30Hz.
5) Lab conditions.

Finally, fracture paths have been analysed by means of a SEM in order to evaluate the loading conditions influence.

RESULTS AND COMMENTS

LOM observations show a traditional structure whose grain diameter mean value is about 700 μm. Alloy microstructure is not completely homogeneous and grains are characterized by a needle like morphology as shown in Fig. 1.

Figure 1: Etched surface of the investigated material.

Needles microstructure is oriented: needles only partially cover the diameter of the prior austenitic grains. No subgrains are observed.
The alloy inhomogeneities have been highlighted by crono-amperometric tests which the results are shown in Fig. 2a [9]. The electrochemical behaviour is characterized by a decrease of current due to presence of corrosion products on the etched surface and to the consequent lower passive property. Corrosion products are not homogenous due to the microstructure differences between grains bulk and boundary.

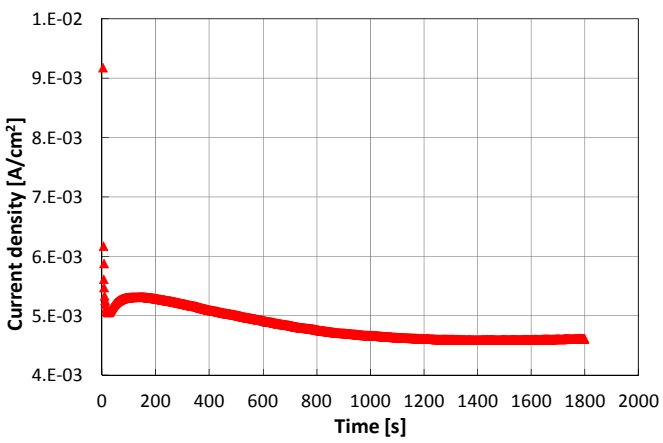

a)

b)

Figure 2: Electrochemical behavior and microstructure etched of material: a) polarization curve, b) microstructure of boundary grain.

"Acicular like" zones near grains boundaries are shown in Fig. 2b. Evidence of microstructure transitions are in Fig. 3, where two diffractograms show respectively the undeformed and the deformed at ε_{eng} = 5% specimen.

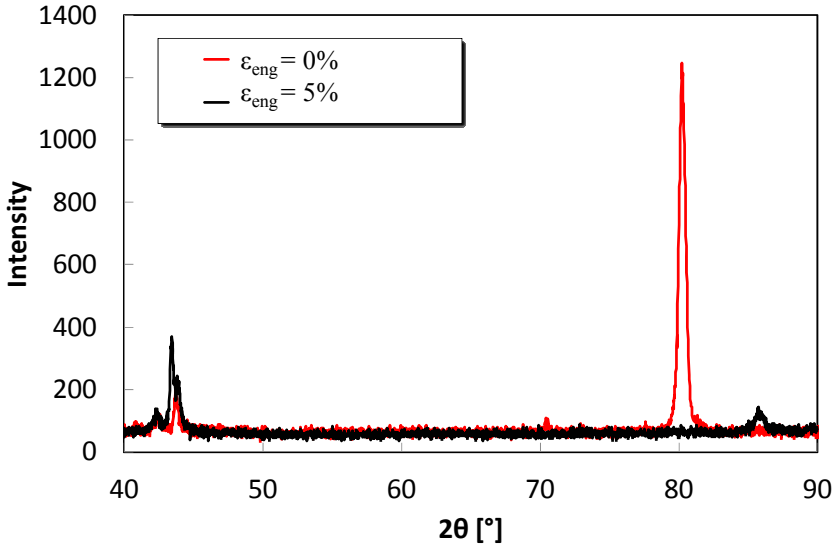

Figure 3: Diffraction spectra.

The undeformed specimen spectrum shows four peaks corresponding to 42.35°, 43.71°, 70.39°, 80.23° that correspond to two different phases [10]:

- Cubic B_2 phase (like CsCl lattice), sometimes named as β_2 that take place at 550°C, but measured peaks are not sufficient to evaluate the cell parameter;
- Cubic L_{21} phase (like Cu_2MnAl), sometimes named as β_3 that take place at 320°C, characterized by cell parameter about a=5.8707 Å.

The ε_{eng} = 5% deformed specimen shows also four peaks but corresponding to different diffraction angles (42.27°, 43.43°, 43.85° and 85.71°). Presence of these peaks are compatible with presence of two phases [11, 12]:

- Austenite β_3 (L_{21} structure not stress induced transformed), characterized by cell parameter about a=5.8707 Å as in the undeformed state.;
- Martensite M18R structure, characterized by a=4.4189 Å, b=5.332 Å, c=38.8 Å and angle β=89.7°.

Peaks modifications (considering both angles and intensity) show the mechanical deformation influence on the microstructure modifications.

Fatigue crack propagation results (da/dN-ΔK) at R=0.1 and R=0.5 are shown in Fig. 4a.

Focusing the R=0.1 results, five different stages can be observed (Fig. 4b). Considering the increase of the crack tip plastic zone radious with the increase of the applied ΔK, a possible crack propagation micromechanism is proposed (to be confirmed by further experimental and numerical analyses):

- stages 1 and 2: the specimen is almost completely austenitic, with the exception of the crack tip plastic zone, but, considering the applied ΔK values, its radious be considered as negligible; corresponding to K_{min} values, considering the typical SMA stress-strain behaviour (Fig. 5), almost all the crack tip plastic zone reverts from martensite to austenite (point A).
- stage 3: transition
- stages 4 and 5: the higher applied ΔK values imply an increase of the radious of the crack tip plastic zone (martensitic!). Corresponding to K_{min} values, the radious of the crack tip plastic zone that does not reverts its microstructure is larger than the one observed in stage 1 and 2 (Fig. 5, point B). In this zone, the stress induced martensite (obtained corresponding to K_{max}) remains unchanged.

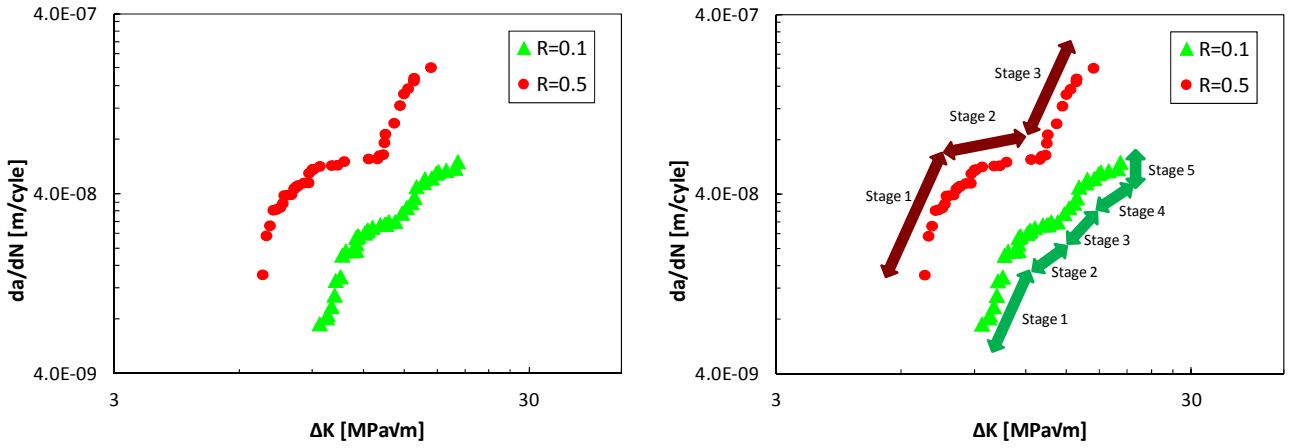

Figure 4: Fatigue crack propagation results: a) da/dN behavior, b) stages.

For R=0.5, only three "traditional" stages are observed. This is probably due to the higher K_{min} values and to the larger extent of the crack tip plastic zone, also corresponding to lower ΔK values, if compared to R = 0.1: martensite obtained corresponding to K_{max} at the crack tip remains unchanged also corresponding to K_{min}.

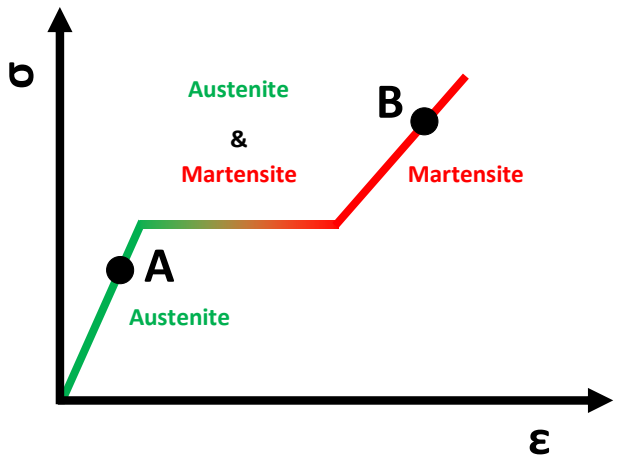

Figure 5: Scheme of σ-ε curve of SMA materials with structure transitions.

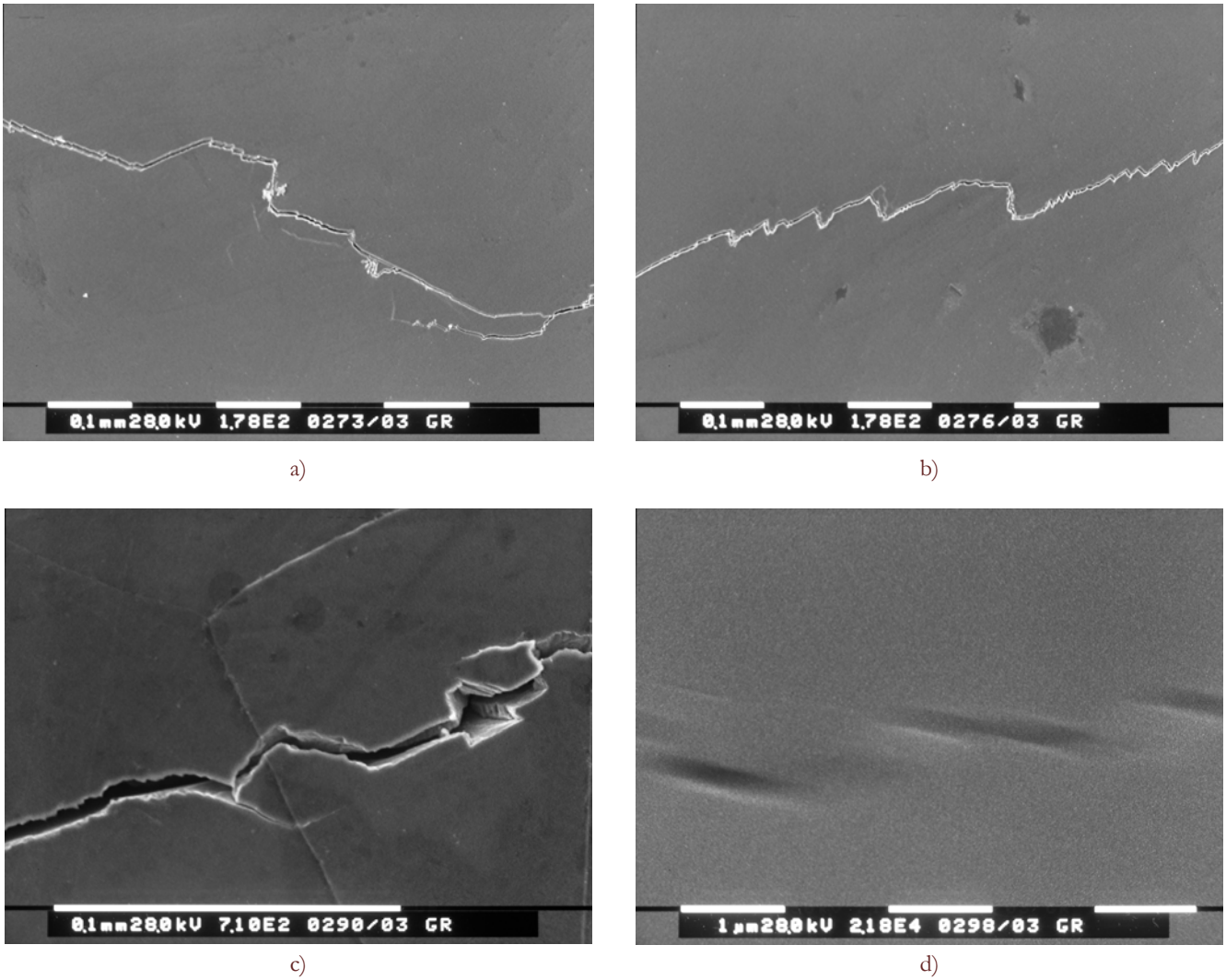

Figure 6: Fatigue crack path at R=0.1: a) and b) two different values of crack extension, c) main and secondary path corresponding to boundary grains, d) high magnification in a zone in the front of conventional crack tip.

For R = 0.1, the crack path is characterized both by the presence of linear paths (Fig. 6a) and by the presence of a sort of "zig-zag" propagation paths (Fig. 6b), with secondary paths that after some hundreds of microns join again the main crack. Presence of "zig-zag" paths are probably due to presence of inhomogeneities boundary grains (brittle precipitates) as shown in Fig. 2b. Secondary crack paths are due to a different interaction of main path to boundary grains, as shown in Fig. 6c. In this case, the main crack is almost to 90° respect the boundary grain and the brittle precipitates deviate the path with an angle that that is analogous to the precipitates angle observed in Fig. 2b. Finally, short microcracks are observed ahead of the crack tip under loading conditions (Fig. 6d), probably due to the stress field around the crack and the consequent microstructure stress-induced transformation.
Considering R=0.5, analogously to the results obtained for R = 0.1, crack paths (Fig. 7a and b) are characterized by the presence of the "zig-zag" path propagation and by the presence of secondary cracks that can be observed at boundary grains (Fig. 7c). The main differences can be summarized as follows:
- Microcracks are not observed ahead of the crack tip. This is probably due to the absence of stage 4 and the crack tip stress field generate a transformed structure characterized by a homogenous behaviour;
- Secondary cracks do not join again the main crack (Fig. 7d).

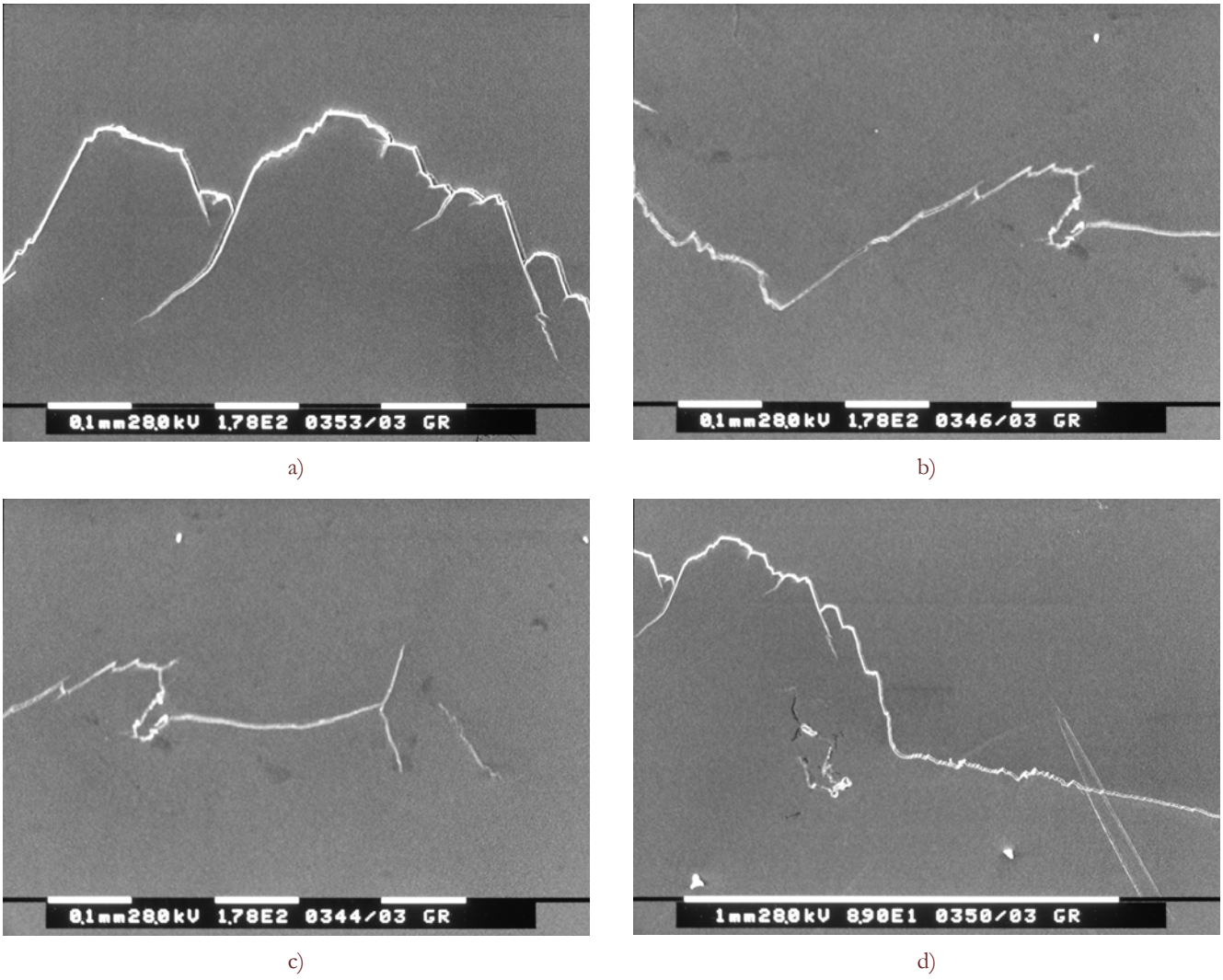

Figure 7: Fatigue crack path at R=0.5: a) and b) two different values of crack extension, c) a zone in the front of conventional crack tip, d) damaged zone near the main crack path.

CONCLUSIONS

In this work, the fatigue crack propagation in a Cu-Zn-Al shape memory alloy, obtained in laboratory, has been evaluated in correlation to main crack micromechanisms by using Scanning Electron Microscopy. Fatigue crack propagation has been carried out by means of traditional hydraulic fatigue crack machine tests and CT specimens, at ΔP=constant, R=0.1 and R=0.5 in lab conditions (ASTM E 647).

For R=0.1, the ability for material to change its structure under load generates a particular fatigue crack propagation behavior characterized by five different stages. Corresponding to the third stage, microstructure transformation takes place.

Considering the crack paths, the following conclusions can be summarized:

1) da/dN-ΔK results are strongly influenced by the R value, probably due to peculiar mechanical behavior of the investigated alloy, with a possible reversion of the stress induced martensite (obtained for K_{max}) to austenite, depending on the loading conditions (R and ΔK values)
2) main crack path is characterized by the presence of a "zig-zag" path, probably due to the presence of brittle inhomogeneities at boundary grains; the angle between main crack and boundary grains determine the initiation of secondary cracks;

3) for R = 0.1, corresponding to "Stage 4", a stress induced microstructure modification is obtained as a consequence of the crack tip stress field, with the consequent initiation of very short microcracks;
4) For R=0.5, no microcracks are observed ahead of the crack tip;
5) For R=0.5, Secondary cracks do not join again the main crack.

REFERENCES

[1] Dong, Y., Boming, Z., Jun, L., A changeable aerofoil actuated by shape memory alloy springs, Materials Science and Engineering A, 485 (2008) 243–250.
[2] Otsuka, K., Ren, X., Physical metallurgy of Ti–Ni-based shape memory alloys, Progress in Materials Science (2005) 511.
[3] Chen, B., Liang, C., Fu, D., Pitting corrosion of Cu-Zn-Al shape memory alloy in simulated uterine fluid, J. Mater. Sci. Technology, 21(2) (2005) 226-230.3
[4] Liu, Y., Tan, G.S., Formation of interfacial voids in cast and micro-grained γ'-Ni3Al during high temperature oxidation, Intermetallics (2000) 8 1385-1391.4
[5] Suzuki, T., Kojima, R., Fujii, Y., Nagasawa, A., Acta Metall., 37 (1) (1989) 163–168.3
[6] Asanovic, V., Delijic, K., Jaukovic, N., A study of transformation of β-phase in Cu-Zn –Al shape memory alloys, Scripta Materialia, 58 (2008) 599-601.7
[7] Kayali, N., Ozgen, S., Adiguzel, O., Strain effects on the macroscopic behaviour and martensite morphology in shape-memory CuZnAl alloys, Journal of Materials Processing Technology, 101 (2000) 245-249.6
[8] Zhang, J.X., Zheng, Y.F., Zhao, L.C., The structure and mobility of intervariant boundaries in 18R martensite in a Cu-Zn-Al alloy, Acta mater., 47(7) (1999) 2125-2141.
[9] Di Cocco, V., Iacoviello, F., Tomassi, L., Rossi, A., Natali, S.,Volpe, V., Crack path in a Zn-Cu-Al PE alloy under uniaxial load, Convegno Nazionale IGF XXII, Roma, Italia, 1-3 Luglio 2013, 255-261, Acta Fracturae ISSN 2281-1443.
[10] Rapacioli, R., Ahlers, M., Ordering in ternary β CuZnAl alloys, Scripta Met., 11 (1977) 1147-1150.
[11] Chandrasekaran, M., Cooreman, L., Yan Humbeek, J., Delaey, L., Martensitic transformation in Cu-Zn-Al: changer in transformation entropy due to post-quench ageing in the β or martensitic condition, Scripta Met., 23 (1989) 237-239.
[12] Wang, T.M., Wang, B.Y., Feng, B.X., Liu, C.L., Jiang, B.H., Xu, Z.Y., the recovery behavior of quenched-in vacancies in Cu-Zn-Al alloy, Phys. Stat. Sol., 114 (1989) 451.